

Overweight and structural alterations of the liver in female rats fed a high-fat diet: A stereological and histological study

Yüksek yağlı diyetle beslenen dişi sıçanlarda ağırlık artışı ve karaciğerin yapısal değişiklikleri: Stereolojik ve histolojik bir çalışma

Berrin Zuhul ALTUNKAYNAK, Elvan ÖZBEK

Department of Histology and Embryology, Atatürk University, School of Medicine, Erzurum

Background/aims: The aim of the present study was to investigate the effects of a fatty diet on body weight and liver morphometry in rats via modern stereological methods accompanied by a histological evaluation. **Methods:** Eight female "Sprague Dawley" rats were fed a diet constituted highly of fat (30%) for 3 months (the HFD group). Eight control rats were maintained with a standard rat chow. The naso-anal length and body weight of the animals were measured periodically to calculate body mass index. After 3 months, whole livers from the rats were removed, and the volume of each fresh liver was estimated using the water immersion method. After the histological procedure, the volume of paraffin-embedded livers was also estimated using the "Cavalieri" method. Additionally, volumes of the sinusoids and parenchyma were separately estimated with "Cavalieri" method. The mean numerical density, mean nuclear height, and total number of hepatocytes were calculated using the physical disector method. Liver sections were also examined at light and electron microscopic levels. **Results:** The body mass indexes of the animals in the control and HFD groups were $4.536 \pm 0.221 \text{ kg/m}^2$ and $5.581 \pm 0.42 \text{ kg/m}^2$, respectively ($p < 0.01$, Mann-Whitney U test). The mean liver volumes (LVs) measured with water immersion method in the control and HFD groups were 10.51 ml and 11.8 ml, respectively. LVs estimated with "Cavalieri" method were 9.98 ml in the control group and 11.095 ml in the HFD group. The differences in LVs between groups were statistically significant when estimated with both methods, indicating that the LV of the HFD group is higher than that of the control group ($p < 0.05$, Mann-Whitney U test). There was no significant difference between LVs estimated via the two different methods in each group ($p > 0.05$, Wilcoxon test). The volume of sinusoids was increased in the HFD group, but the volume of parenchyma was decreased ($p < 0.05$, Mann-Whitney U test). The mean numerical density, mean nuclear height, and total number of hepatocytes were significantly decreased in the HFD group ($p < 0.05$, Mann-Whitney U test). However, the numerical density and total number of binucleated hepatocytes were significantly higher in the HFD group compared with the control group ($p < 0.05$, Mann-Whitney U test). Light and electron microscopic investigations of the HFD group showed a prominent sinusoidal dilatation, microvesicular steatosis, and an increase in connective tissue in the livers and highly dilated smooth endoplasmic reticulum, irregular mitochondria and microvilli and necrosis in the hepatocytes. **Conclusions:** We have shown that a fatty diet in rats causes obesity and may lead to morphological alterations in the liver such as hepatomegaly accompanied by histopathological changes.

Key words: Fatty diet, hepatomegaly, histopathology, overweight, rat, stereology

Amaç: Bu çalışmanın amacı, yağlı diyetin vücut ağırlığı ve karaciğer morfometrisi üzerine etkilerini, histolojik değerlendirmeye birlikte modern stereolojik yöntemleri de kullanarak sıçanlarda araştırmaktır. **Yöntem:** "Sprague Dawley" cinsi 8 adet dişi sıçan 3 ay boyunca yağ içeriği yüksek (%30) bir diyetle (YYD grubu); 8 adet kontrol sıçan ise standart sıçan yemi ile beslendi. Hayvanların naso-anal uzunluğu ve vücut ağırlığı, "vücut kitle indeksini" hesaplamak için periyodik olarak ölçüldü. Üç ay sonra sıçanların karaciğerleri bütün halinde çıkarıldı ve her bir taze karaciğerin hacmi, "suya daldırma metodu" kullanılarak ölçüldü. Histolojik takipten sonra parafine gömülen karaciğerlerin hacmi, "Cavalieri" metodu ile de hesaplandı. Bunun yanı sıra "Cavalieri" metodu ile, sinüzoidlerin ve parankimanın hacimleri ayrı ayrı ölçüldü. Hepatositlerin toplam sayısı, ortalama nükleus yüksekliği ve ortalama sayısal yoğunluğu fiziksel disektör yöntemiyle hesaplandı. Karaciğer kesitleri ayrıca ışık ve elektron mikroskopik düzeylerde incelendi. **Bulgular:** Kontrol ve YYD grubundaki hayvanların vücut kitle indeksleri sırasıyla $4,536 \pm 0,221 \text{ kg/m}^2$ ve $5,581 \pm 0,42 \text{ kg/m}^2$ idi ($p < 0,01$; Mann-Whitney U test). Suya daldırma metodu ile ölçülen ortalama karaciğer hacimleri, kontrol ve YYD gruplarında sırasıyla 10,51 ml ve 11,8 ml idi. "Cavalieri" metodu ile hesaplanan karaciğer hacimleri kontrol grubunda 9,98 ml ve YYD grubunda 11,095 ml idi. İki grubun karaciğer hacimleri arasındaki fark, her iki metotla da hesaplandığında, istatistiksel olarak önemliydi; yani YYD grubunun karaciğer hacimleri, kontrol grubundakinden daha fazlaydı ($p < 0,05$; Mann-Whitney U test). Her bir grup için de iki farklı metotla hesaplanan karaciğer hacimleri arasında önemli bir fark yoktu ($p > 0,05$; Wilcoxon test). Sinüzoidlerin hacmi YYD grubunda artmıştı, fakat parankima hacmi azalmıştı ($p < 0,05$; Mann-Whitney U test). Hepatositlerin toplam sayısı, ortalama sayısal yoğunluğu ve ortalama nükleus yüksekliği YYD grubunda önemli derecede azalmıştı ($p < 0,05$; Mann-Whitney U test). Ancak iki nükleuslu hepatositlerin toplam sayısı ve sayısal yoğunluğu, kontrol grubuyla kıyaslandığında YYD grubunda önemli derecede daha fazlaydı ($p < 0,05$; Mann-Whitney U test). Işık ve elektron mikroskopik incelemelerle; YYD grubunda karaciğerde belirgin sinüzoidal dilatasyon, mikroveziküler yağlanma ve bağ dokusunda artış gözlemlendi; hepatositlerde oldukça genişlemiş düz yüzü endoplazmik retikulum, düzensiz mitokondriler ve mikrovelluslar ve nekroz saptandı. **Sonuç:** Biz bu çalışmada, yağlı diyetin sıçanlarda obeziteye sebep olduğunu ve karaciğerde histopatolojik bulgularla eşlik edilen hepatomegali gibi morfolojik değişikliklere yol açabileceğini gösterdik.

Anahtar kelimeler: Yağlı diyet, hepatomegali, histopatoloji, ağırlık artışı, sıçan, stereoloji

Address for correspondence: Elvan ÖZBEK
Atatürk Üniversitesi Tıp Fakültesi
Histoloji-Embriyoloji Anabilim Dalı Erzurum, Turkey
Phone: + 90 442 231 65 89 • Fax: + 90 442 236 09 68
E-mail: elvanozbek@yahoo.com

Manuscript received: 23.07.2008 **Accepted:** 19.02.2009

INTRODUCTION

Today, the prevalence of obesity has reached epidemic levels in most developed countries, especially in the United States (1). Obesity is a growing problem in modern societies due to the intensive lifestyle, high carbohydrate or fat dietary intake, and reduced energy consumption. More than half of adult Americans are overweight today (2). Obesity is generally responsible for many chronic diseases such as cardiovascular problems, hypertension, diabetes, and hyperlipidemia (1). Additionally, obesity is the most important risk factor for complex and chronic liver disorders (3). These liver disorders begin as steatosis and may progress to steatohepatitis, cirrhosis, liver failure, and hepatocellular carcinoma (4, 5). It has been previously reported that insulin-resistant type 2 diabetes and hyperlipidemia occur in most liver cases (6). Although there are no apparent symptoms, some disorders such as hepatomegaly, abnormal liver biochemistry and abdominal ultrasound findings can be incidentally determined in patients with liver diseases (7).

Stereology is a series of tools used to quantify features of 3D objects from their 2D sections through an object (such as microscopic slides of a solid specimen). The specialization of stereological tools makes these estimates unbiased and reliable (8, 9).

In the practice of stereology, we place test devices (grids, points, lines) over planes cut through our specimens (histological or magnetic sections). The geometric properties of the test systems are known (10, 11). Therefore, we can get information about unknown properties of our specimens by observing how the test devices relate to them. This quantitative information supplies an important contribution to biomedical research by exploiting the constancy and integrity of results performed in the laboratories of basic and clinical departments and reported in scientific journals.

While various diagnostic approaches have been used to evaluate liver diseases in obese patients (12), very few stereological studies have been performed till now to estimate the quantitative changes in the liver (13, 14). Moreover, only one of these studies reported the effects of a high-fat diet on liver stereology (15).

The aims of the present study were as follows: 1) to form an obesity model by feeding rats with a high-fat diet, 2) to evaluate possible quantitative changes in the livers of obese rats by estimating

the volumetric data via both the water immersion method (WIM) and the unbiased Cavalieri method (CM) and numerical data via the physical disector method, and 3) to examine microscopically the anatomy of the livers of obese rats to determine possible histopathological changes.

MATERIALS AND METHODS

Animals and Diets

Sixteen adult female *Sprague Dawley* rats (150-200 g each) from the Experimental Research and Application Center of our university were randomly allocated into two groups of equal number. The control rats were fed a commercial rat diet (7-10% fat, 68-70% carbohydrates, 18-20% protein, 1-2% vitamins and minerals; 210 kcal/100 g/day) for 3 months, while rats in the treatment group (the HFD group) were fed a high-fat diet (30% calories as fat) for the same period of time. To prepare the fatty diet, the commercial rat diet in powder form was mixed with melted animal abdominal fat so as to provide 30% of the total energy from fat. This mixture in a dough-like consistency was given a shape like that of the commercial rat diet, and dried, and used for feeding animals in the treatment group.

The rats were housed in plastic cages (2 animals per cage), maintained under standardized conditions of light (12-h light/dark cycle) and room temperature ($22\pm 2^\circ\text{C}$), with free access to food and tap water. The diet consumption of all animals was monitored daily, and the animals were weighed at the beginning of the study and once every 10 days for 3 months to determine any weight increase. At the end of the experiment, the animals were anesthetized with Sevoflurane[®] (Abbott, Ultane; Canada), and their naso-anal length was measured to calculate the body mass index [$\text{BMI} = \text{weight (kg)} / \text{length (m)}^2$]. Subsequently, the anesthetized animals were sacrificed by intracardiac perfusion of 10% formalin solution. Whole livers were removed from the rats and processed for stereological and microscopic analyses (Figure 1). This study was given ethical approval by the Experimental Research and Application Center.

Tissue Processing for Stereological and Light Microscopic Analyses

To detect the volume of the whole liver (LV), the removed fresh livers were first immersed in water, and the LVs were measured using WIM (Figures 1A and 1B). Then, livers were systematically and

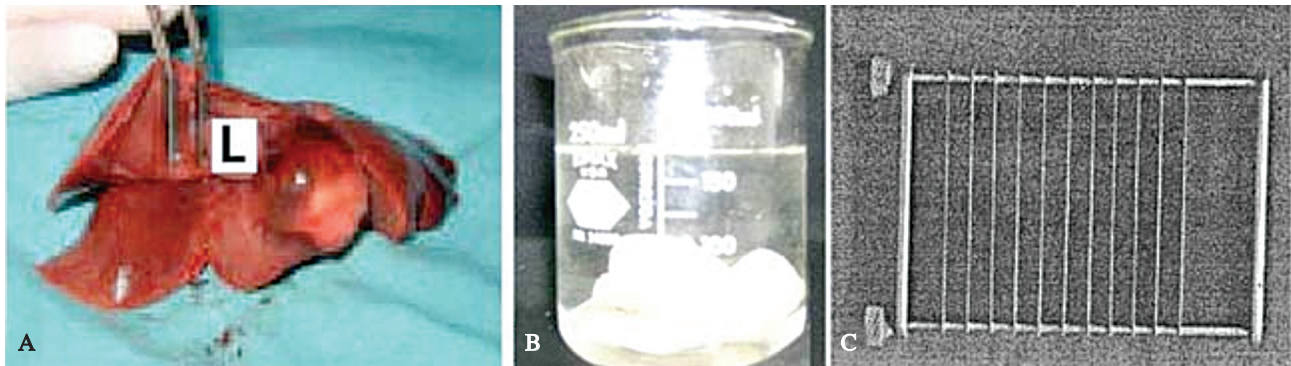


Figure 1. A. Removed whole liver, B. Volumetric estimation in water, C. Fractionating knives.

randomly sampled using fractionating knives (Figure 1C) for stereological evaluation. The livers were cut into 5- μm slices with these knives, and 6-8 liver pieces were obtained from each liver. On the basis of a pilot study, it was decided to select every 5th liver piece from all the pieces (Figure 2A) (16). Following this step, selected pieces were cut into tissue cubes with the knives, and every 5th tissue cube was selected from all cubes. Thus, three liver cubes at 125 mm³ were used for final estimations.

Subsequently, selected liver cubes from each liver (Figure 2B) were post-fixed in 10% formalin solution for 48-55 hours, dehydrated in graded alcohol series, embedded in paraffin wax, and serially sectioned using a *Leica RM2125RT* microtome (Leica; Germany). Serial sections of 5 μm thickness were mounted on glass slides. As the second step of the stereological procedure, every 5th liver section was selected through a set of consecutive paraffin sections from each selected liver piece. The first section was chosen randomly. Fifteen to 20 sections were sampled from each rat liver in a systematic random manner (17). Selected sections were stained with hematoxylin-eosin (H&E), and photographed on the PC screen (Figure 2C) using a light microscope (Olympus BH-2; Japan) with a digital

color camera attachment (Sanyo VVC-6975P; Japan) and dial indicator. The unbiased CM was applied to the light microscopic images for the stereological estimation of LV, and the volume of the sinusoids and the parenchyma (18, 19).

Thus, three different point-counting test grids were used to estimate the sectioned area in the liver (Figure 2D). These grids were used to estimate the volume of the liver (Figure 2D), the volume of sinusoids, and the volume of the parenchyma, respectively. The point density of the point-counting grids was designed to obtain an appropriate coefficient of error (CE) for an area of interest in images of the serial sections (19, 20). The CE and coefficient of variation (CV) were estimated according to Gundersen and Jensen's formula (21-23). The test grid with a systematic array of points was randomly placed on the screen of the PC, and the estimation area was sampled in a 1/4 ratio according to the optimal CE. The volume of each area of interest (only sinusoids or parenchyma) in all liver sections was estimated using the following formula:

$Volume = t \times a/p \times \Sigma P$ ("t", section thickness; "a/p", representing the area of each point on the point-counting grid; " ΣP ", total number of the points hitting the area of interest)

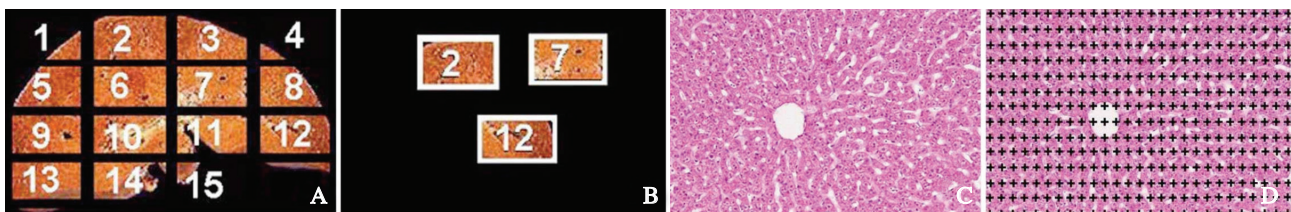


Figure 2. A. Selected liver slices from a whole liver. B. Selected liver pieces from each liver slice. C. A light microscopic image from a selected liver section (x10 magnification). D. Light microscopic image at A after superimposing a point-counting grid (x10 magnification).

Then, the total volume of the selected sections from each rat liver was multiplied by 125 (total fraction ratio) to estimate LV (LV= total volume of selected sections x 5 x 5 x 5), total sinusoid volume, and the volume of the parenchyma.

Sample estimation for the LV was performed as follows:

$$\text{Volume} = (t \times a/p \times \Sigma P) \times A \text{ (area sampling ratio)} \times 125 \text{ (tissue sampling ratio)}$$

$$\text{Volume} = (0.0005 \times 0.0625 \times 620) \times 4 \times 125$$

$$\text{Volume} = 9.69 \text{ cm}^3$$

For light microscopic examination, sections were stained with three different histochemical methods, H-E, Oil Red O stain, and Von Gieson technique (24). Slides were covered and photographs taken using a light microscope with a camera attachment (Nikon Eclipse E600; Japan).

Number of Hepatocytes:

The sampling of physical disector pairs was done as described previously (23). In brief, we obtained approximately 180 sections from each liver. According to our preliminary study, the pairs from every 9th section were chosen randomly, and in this way, approximately 15-20 section pairs were obtained. It has been reported that this number is in an acceptable range for stereological analysis (21-23). Disector pairs were taken from the tissue at a known interval (1/5), until the tissue sample was exhausted. Two consecutive sections were mounted on each slide. Photographs of adjacent sections were taken with a digital camera (Olympus BH-2; Tokyo, Japan) at a magnification of x400. If a hepatocyte nucleus was seen in the reference section but not in the look-up section, it was counted as a disector particle (22). To increase the countable disector particle number, i.e., the nucleus, we exchanged the role of sections in the second step. An unbiased counting frame was placed on the reference and the look-up sections on the screen of the PC to perform the counting according to the disector counting method (8, 22). In these disector pairs, one-nucleated and binucleated hepatocytes were considered at x20 objective and x400 final magnification. Firstly, the numerical density of all hepatocytes (one- and two-nucleated) was estimated, and then, the numerical density of only binucleated hepatocytes seen in the same disector pairs was estimated.

The mean numerical density of hepatocytes (one- and two-nucleated) (NV(HC)) per cm³ was estimated using the following formula:

$$Nv_{(HC)} = \Sigma Q^-_{(HC)} / t \times af$$

Where $\Sigma Q^-_{(HC)}$ is the total number of nuclei seen in the reference but not in the look-up section, "t" is the mean section thickness (5 μ m), and "af" is the area of the unbiased counting frame.

In another step of this study, the mean nucleus height was estimated to comment about the hepatocyte size.

The mean nucleus height ($H_{(nucleus)}$), which is an estimation of the size of the nucleus, was estimated using the following equation (20,25).

$$H(nucleus) = \left[\frac{\Sigma Q_{(nucleus)}}{\Sigma Q^-_{(nucleus)}} \right] \times t$$

Where $\Sigma Q_{(nucleus)}$ is the total number of nuclei seen in the reference section, $\Sigma Q^-_{(nucleus)}$ is the total number of disector nuclei seen in the reference but not seen in the look-up section, and "t" is the mean section thickness (5 μ m). The total number of HC ($TN_{(HC)}$) in the rat liver was estimated by the following equation:

$$TN_{(HC)} = Nv_{(HC)} \times LV$$

Where $Nv_{(HC)}$ is the numerical density of hepatocytes (NV(HC)) in cm³ and LV is the liver volume (cm³) estimated using the Cavalieri principle.

Correction for Tissue Shrinkage:

Shrinkage will affect all stereological size estimators including volume (26, 27). Measurements were made to quantify shrinkage caused by fixation and histological procedures. For this purpose, the volume of removed fresh liver was calculated by WIM. After processing and exhaustively cutting, the LV was estimated with the CM (21). The volume shrinkage was then calculated as follows:

$$\text{volume shrinkage} = 1 - \left[\frac{\text{volume after}}{\text{volume before}} \right]$$

Stereo Investigator:

The physical disector was used to estimate the numerical density of hepatocytes and the CM to estimate the LV by means of a workstation, made with a microscope (Olympus BH-40; Tokyo, Japan) equipped with a matching condenser, a microcator (LEP Electronic Products Ltd; Hawthorne, NY, USA) to control the movements in z-axis (accuracy 0.5 μ m), a motorized stage for stepwise displacement in the x-y axis (accuracy 1 μ m), and a CCD video camera (Sony; Tokyo, Japan) connected to a 21-inch PC monitor (Philips). The whole system was controlled by the software Stereo Investigator

(MicroBrightField Inc.; Wiliston, VT, USA; version 6.0).

Electron Microscopic Procedure:

For the electron microscopic examination, livers were fixed in 3% glutaraldehyde in 0.1 M phosphate buffer, post-fixed in 1% osmium tetroxide in 0.1 M phosphate buffer, dehydrated in a graded acetone series, and transferred to propylene oxide. After dehydration, specimens were embedded in Araldite CY 212. Sections were cut using an ultramicrotome (LKB NOVA, Bromma, Sweden). Then, ultra-thin sections were stained with uranyl acetate and lead citrate. Finally, sections were examined under a Jeol 100 SX electron microscope (Jeol; Tokyo, Japan).

Histopathological examinations were carried out on the images of the same sections at both light and electron microscopic levels.

Statistical Analyses:

Microsoft® SPSS Version 13.0 for Windows was used for statistical analyses. The Mann-Whitney U test was applied to compare the control and treatment groups with respect to BMIs, volumes of the liver and the sinusoids, the mean volume of the hepatocytes and the mean numerical density, and the total number and mean nuclear height of the hepatocytes. Differences between the two methods used for estimating LVs were analyzed in each group and between groups using the Wilcoxon signed-ranks test. All statistical values under 0.05 were considered significant.

RESULTS

In the present study, no animals died in either group during the experiment. The BMI results are summarized in Figure 3. The mean BMI was 4.536 ± 0.221 kg/m² in the control group and 5.581 ± 0.42 kg/m² in the HFD group. The difference between

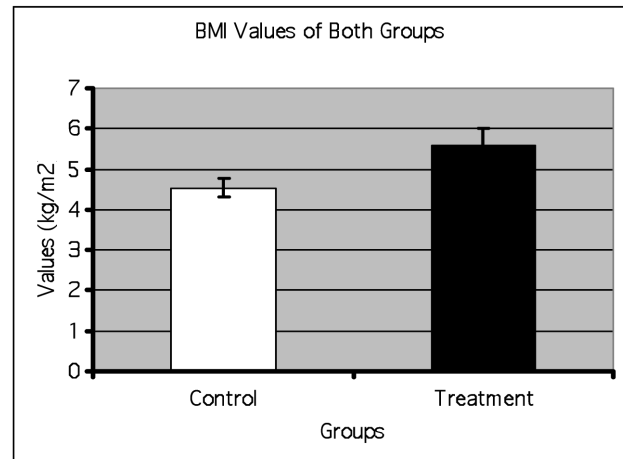


Figure 3. BMI (body mass index) values of animals in both groups (Mean \pm SEM).

the BMI values of the two groups was statistically significant ($p < 0.01$, Mann-Whitney U test).

The LVs of the control and HFD groups were significantly different from each other when estimated with both WIM and CM, suggesting that the LV of the rats in the HFD group is higher than that in the control group ($p < 0.05$, Mann-Whitney U test) (Table 1). However, there was no statistically significant difference between LVs estimated via the two different methods in each group ($p > 0.05$, Wilcoxon test), indicating that CM is as safe as WIM for estimations. Also, the volumes of the sinusoids in the two groups were different ($p < 0.05$, Mann-Whitney U test) (Table 1). The volume of the parenchyma in the control rats was higher than in the HFD group ($p < 0.05$; Mann-Whitney U test) (Table 1).

The tissue shrinkage ratio was estimated as 5.1% in the control group and 6% in the HFD group, and the shrinkage ratios were not significant in either group ($p > 0.05$; Mann-Whitney U test). Also, there

Table 1. Morphometric evaluations performed in this study

Measurements	Control Group (\pm SEM)	CE	HFD Group (\pm SEM)	CE
LV via WIM (cm ³)	10.51 \pm 1.3	-	11.8 \pm 1.77	-
LV via CM (cm ³)	9.98 \pm 1.21	0.002	11.095 \pm 3.11	0.002
Volume of parenchyma (cm ³)	6.702 \pm 1.34	0.012	5.408 \pm 1.17	0.023
Volume of sinusoids (cm ³)	3.278 \pm 0.87	0.031	5.687 \pm 1.76	0.029
MND of hepatocytes (cell/cm ³)	204,820,000 \pm 1,428,406	0.012	177,750,000 \pm 1,297,210	0.017
MND of binucleated hepatocytes (cell/cm ³)	23,523,000 \pm 832,145	0.042	32,540,000 \pm 643,890	0.038
TN of hepatocytes	2,044,103,600 \pm 123,425,678	0.029	1,772,136,250 \pm 109,247,689	0.046
TN of binucleated hepatocytes	234,759,540 \pm 17,178,912	0.021	361,031,300 \pm 28,790,121	0.032
NH of hepatocytes (μ m)	6.34 \pm 0.81	0.037	5.22 \pm 0.44	0.043

LV: Liver volume. WIM: Water immersion method. CM: Cavalieri method. MND: Mean numerical density. TN: Total number. NH: Nuclear height. CE: Coefficient of error. SEM: Standard error mean.

was no significant difference in terms of tissue shrinkage between the two groups ($p > 0.05$, Mann-Whitney U test).

The mean numerical density of hepatocytes in each group is shown in Table 1. The numerical density of hepatocytes in the livers of the HFD group was significantly decreased (about 13.3%) in comparison to the control group ($p < 0.001$). However, the mean numerical density of binucleated hepatocytes was significantly increased (about 38.33%) compared to the control group ($p < 0.0001$) (Table 1).

The total number of hepatocytes in the livers of the control and HFD groups is shown in Table 1. The total number of hepatocytes in the livers of the HFD group was significantly decreased compared to the control group ($p < 0.001$). However, the total number of binucleated hepatocytes was significantly increased ($p < 0.001$) in the livers of the HFD group compared to those of the control group (Table 1).

The mean nuclear height of the hepatocytes of the HFD and control groups is shown in Table 1. There was a significant difference between the mean nuclear heights of the hepatocytes of the HFD and control groups ($p < 0.001$). The mean nuclear height

of the hepatocytes in the HFD group was 17.7% lower than the mean nuclear height of the hepatocytes in the control group.

By light microscopy of the livers from the HFD group, prominent dilatations were observed in the sinusoidal capillaries and central veins and branches of the portal vein (Figures 4B, 4F). In the Oil Red O-stained slides of the HFD livers, many more red droplets within the cytoplasm of hepatocytes were present in comparison with the control livers (Figures 4A, 4C, 4E), indicating microvesicular steatosis in the livers of the HFD group (Figure 4F), and many hypertrophied hepatocytes containing large cytoplasmic vacuoles were found (Figure 4F right inset). Additionally, there were red-colored areas around the portal triad in the Von Gieson-stained liver sections of the HFD group, showing an increased fibrosis (Figure 4D). Cell plates consisting of eosinophilic hepatocytes with dense cytoplasm and dark nuclei were also seen, suggesting a cellular degeneration leading to necrosis (Figure 4B). Necrotic foci (Figure 4B and right inset in 4B) accompanied by mononuclear cell infiltrations and fibrotic areas (Figure 4B and left inset in 4B), and many macrophages (Figure 4F) were found in the liver sections of the HFD group.

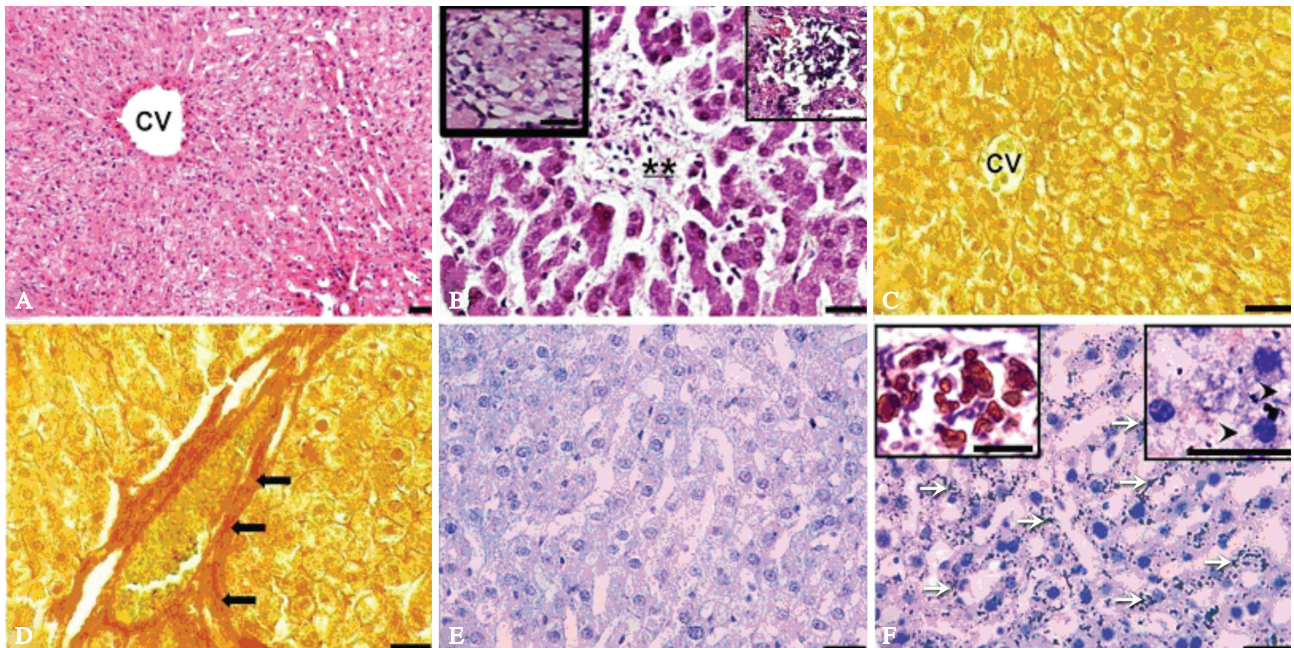


Figure 4. A, B, C, D, E and F: Light micrographs of livers from the control (A, C and E) and HFD (B, D and F) groups. CV, central vein; CT, connective tissue; **Asterisks** indicate a necrotic focus containing fibrotic areas and mononuclear cells; **Black arrows**, connective tissue enlargement at perivascular areas; **White arrows** show microvesicular lipid droplets within the hepatocytes. **Insets** in B show fibrotic (on left) and necrotic (on right) areas with mononuclear cell infiltrations. **Insets** in F reveal macrophages (on left) and hypertrophied hepatocytes undergoing ballooning degeneration (on right, arrow head). **Stains:** Hematoxylin-eosin (A, B); Von Gieson (C, D); Oil Red O (E, F). Magnification Bars: 60 μm .

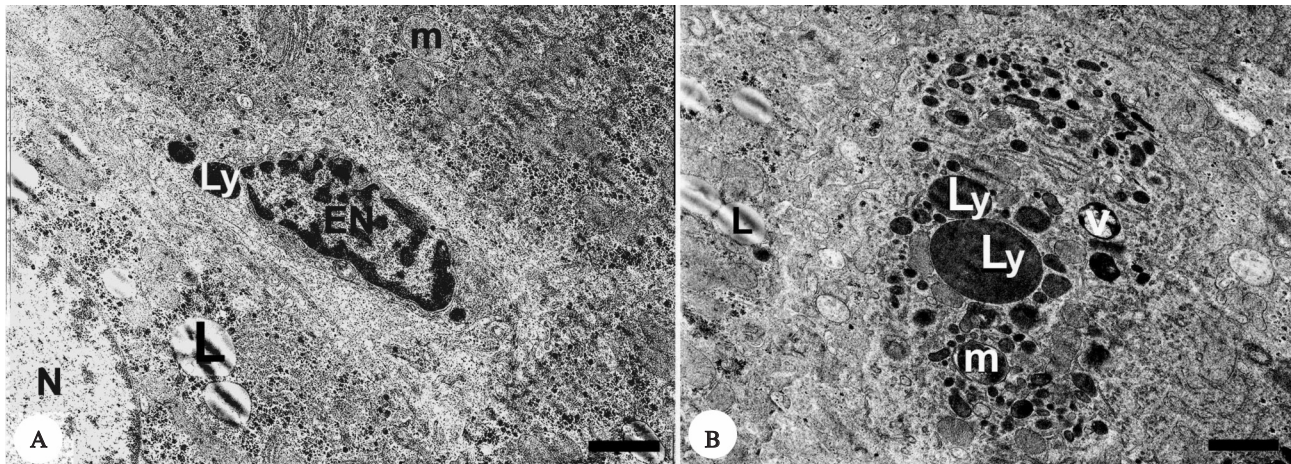


Figure 5. A and B: Electron micrographs of livers from the HFD group; **EN**, condensed nuclei of endothelium; **ly**, lysosomes; **L**, lipid droplet; **m**, mitochondrion; **N**, nucleus of hepatocyte; **v**, vacuole; a Kupffer cell filled with lysosomes and vacuoles is seen in **B**. **Stains:** Uranyl acetate and lead citrate. **Magnification Bars:** 1 μm .

In the electron microscopic sections of the livers from the HFD group, chromatin condensation of the endothelial cell nuclei (Figure 5A) and numerous lipid droplets within the hepatocytes (Figures 5A, 6B) were observed. In both hepatocytes and Kupffer cells, abundant lysosomes were present (Figures 5B, 6A). The boundaries of mitochondria were irregular, and the mitochondrial contents were dispersed in the cytosol (Figures 6B, 6B-inset, 7A-inset). The smooth endoplasmic reticulum was dilated and enlarged, and the microvilli were irregular and

smooth and abnormally protruded in some spots in the hepatocytes of the HFD group (Figure 7B).

DISCUSSION

Weight gain and obesity are major risk factors for conditions and diseases ranging from insulin resistance and type 2 diabetes mellitus to atherosclerosis (28). The prevalence of liver disorders is high in obese people, and in patients who have type 2 diabetes-mellitus, insulin resistance is one of the key elements leading to liver disease in obese people

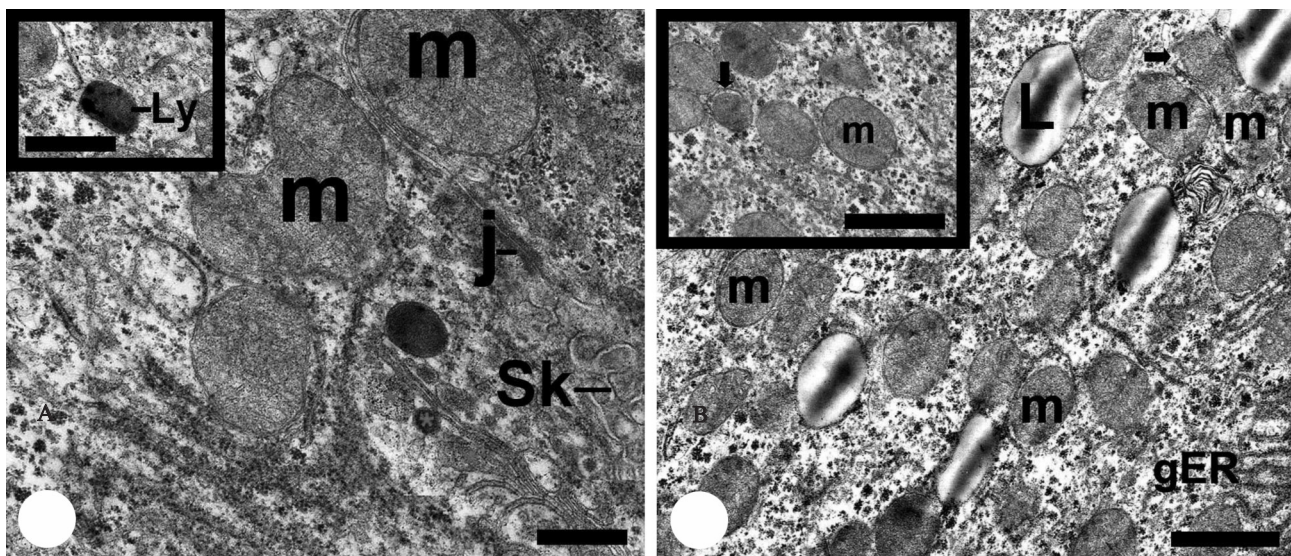


Figure 6. A and B: Electron micrographs of livers from the HFD group. **M**, mitochondrion (giant ones in **A**); **sk**, bile canaliculi; **j**, intercellular junction; **inset in A** shows a secondary lysosome; **gER**, rough endoplasmic reticulum; **L**, lipid droplet; **inset in B** reveals mitochondria; **black arrows** show degenerated mitochondria. **Stains:** Uranyl acetate and lead citrate. **Magnification Bars:** 1 μm .

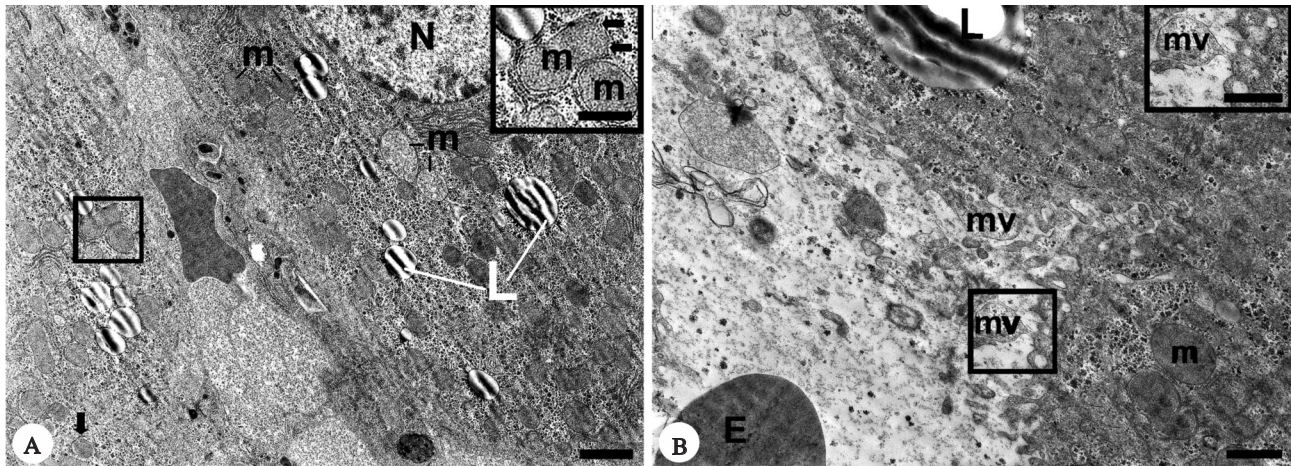


Figure 7. A and B: Electron micrographs of livers from the HFD group. **N**, hepatocyte nucleus; **m**, mitochondrion; **L**, lipid droplet; **inset in A** shows mitochondria with irregular boundaries (arrow heads) at high magnification of boxed area in **A**; **mv**, microvillus; **inset in B** reveals an irregular protrusion of microvillus. **Stains:** Uranyl acetate and lead citrate. **Magnification Bars:** 0.8 μm .

(29). These are often asymptomatic in the absence of decompensated cirrhosis, but should be suspected in patients with elevated aminotransferase levels or radiological evidence of a fatty liver or hepatomegaly (30). Liver biopsy is the only way to assess the histological features of necrotic inflammation and fibrosis that define nonalcoholic steatohepatitis and to determine its probable prognosis (31).

Stereological procedures are efficient methods, if you want to obtain quantitative analyses and interesting volume of objects in any biological tissue or organ. However, stereological procedures can often be boring, complex, and confusing. Thus, stereological studies are not easy at all times. If stereological software such as Stereo Investigator is used, it gives more dependable results by eliminating the confusion and renders the complex parts of the stereological methods for the user so that significant analyses can be done quickly and easily. The stereological methods and Stereo Investigator used in our study involve a hierarchy of systematic random sampling combined with the Cavalieri and physical disector methods (13, 20)

Although much useful information has been obtained to date from different types of studies, such as structural (32), ultra-structural (33) and clinical (29), about the effects of a high-fat diet on the rat liver, there is only one study in the literature using stereological methods (15).

In this study, the effects of a high-fat diet on the morphometry and histology of the liver were detailed in a female rat model.

The difference between the WIM-calculated liver volumes of the control and HFD groups was significant ($p < 0.05$, Mann-Whitney U test). The WIM-measured values have undoubtedly indicated a hepatomegaly in the HFD group. They are certain results, not estimated because they were calculated by overflowing water. The difference between the CM-estimated liver volumes of the control and HFD groups also suggested a hepatomegaly ($p < 0.05$, Mann-Whitney U test) and has thus supported the WIM results. According to the statistical analyses, tissue shrinkage was not important in either the control or the HFD group ($p > 0.05$, Wilcoxon test).

It was clearly defined that volumetric calculations using WIM give the closest results to real volumetric values. In experimental studies, the liver is easily removable from animals. But in human subjects, it is impossible, and liver volume can be unbiasedly estimated by using CM on either biopsy materials or magnetic resonance (MR) images. The results of this study suggest that volumetric estimations using CM are obviously reliable, and similar to those using WIM.

When these results were evaluated from different aspects to take into account the mean liver volume / mean body weight, more dramatic data were obtained. There was a significant difference ($p < 0.001$, Mann-Whitney U test) between the “mean liver volume / mean body weight” values of the control and HFD groups, indicating that it may be more useful to evaluate volumetric changes in the liver and body weight together.

The volume of sinusoids was significantly increased in the livers of the HFD-fed rats. The reason for this increase may be the sinusoidal dilatation observed histologically. However, the volume of the parenchyma was significantly decreased due to necrosis. The numerical density of hepatocytes was decreased in the HFD group, and the total number of hepatocytes was lower in the HFD group than in the control group because of the parenchymal loss following the necrosis.

Cell size is related to ploidy because a polyploid cell has more chromatin and thus is larger than a diploid cell (34). Also, the number of binucleated hepatocytes increases in conjunction with age (35, 36). However, the high population of binucleated hepatocytes is one criterion for chronic liver disease, including hepatitis, cirrhosis, diabetes or cancer (37). In this study, we estimated that the numerical density of binucleated hepatocytes was approximately two times higher in the livers of rats from the HFD group than in those of the control rats. The total number of binucleated hepatocytes was also higher in the HFD group than in the control group. In the present study, we thought the higher number of binucleated hepatocytes observed in the HFD group might have been the result of a compensatory mechanism in response to the decreased number and size of hepatocytes in that group due to necrotic changes.

Mean nuclear height was decreased in the HFD group compared with the control group. During the histological evaluation of the liver sections from the HFD group, many necrotic hepatocytes possessing low nuclear height were observed. This finding is also very important because this is the first study estimating the nuclear height of hepatocytes.

Our microscopic analyses indicated microvesicular fat in the livers of the HFD-fed rats. In previous studies, microvesicular steatosis was found following high methionine-containing diet (38). As shown in our light and electron microscopical findings, after feeding with HFD, mitochondrial alterations in addition to microvesicular steatosis in hepatocytes were determined. Many researchers reported that microvesicular steatosis occurred due to changes in enzyme levels of hepatocytes. They emphasized that it was caused by oxidative stress resulting in mitochondrial degenerations (39). Furthermore, high blood levels of steroids after HFD may have caused microvesicular steatosis in this study.

In the slides of the HFD group, the orientation of the hepatocyte plates was not regular. This event may have occurred as a result of oxidative damage in hepatocellular proteins or necrotic changes in hepatocytes. Abraham et al. (40) (2002) also mentioned a similar finding in their study.

As proved in the present study, we suggest a new finding that notes that feeding with a fatty diet may cause a vascular dilatation in the liver. This dilatation may be caused by inflammatory changes. Similarly, Dai and Chen (41) (2006) reported expanded sinusoids in the livers of HFD-fed rats. This dilatation may also be caused by ischemia and hypoxia following HFD (42, 43). According to different views, vascular dilatation may occur due to developing hypertension after obesity induced by HFD (44, 45).

There are few studies about the effects of a high-fat diet on liver ultrastructure in the literature. In one of these, Dai and Chen (41) (2006) showed that the mitochondria and rough endoplasmic reticulum (RER) expanded and their number increased. This is the first mention in the literature of our ultrastructural findings, such as smoothed or protruded microvilli, irregular degenerated mitochondria, abundant lipid droplets and lysosomes in the hepatocytes and nuclear condensation of endothelial cells in the livers of the HFD group.

Our data suggest three important points: i) Feeding with a high-fat diet (30%) causes obesity, hepatomegaly, and histopathological changes in the liver in female rats. ii) In spite of hepatomegaly, a decrease in the number of hepatocytes in the HFD group was found. iii) In this situation, hepatomegaly in obese rats may be caused by sinusoidal dilatation (increase in volume of sinusoids), microvesicular steatosis, or fibrosis resulting from an increase in connective tissue following hepatocellular necrosis. In this point decreasing nuclear volume sign that cell death, as light microscopically shown.

Today MR- or tomography-based stereology is being used for diagnosis and determining treatment procedure in liver diseases (46, 47). According to our findings, evaluation of volumetric changes with modern stereological methods on serial MR or tomography images obtained from obese patients (BMI>30) can be useful for early diagnosis of non-alcoholic fatty liver disease (NAFLD), which is associated with obesity (19, 23). Thus, before examining the biopsy specimen of the liver, the li-

ver volume of the patients may be estimated on their serial MR or tomography images using the Cavalieri method in terms of both early determination of hepatomegaly and efficiency of the treatment procedure. If it is not possible, physicians must consider hepatomegaly, decreasing hepa-

toocyte activity and inflammation of liver when treating NAFLD and administering drugs to these patients with NAFLD.

Acknowledgement: The present study was supported by the Atatürk University Scientific Research Fund (2005/183-protocol number).

REFERENCES

- Choudhury J, Sanyal AJ. Insulin resistance and the pathogenesis of nonalcoholic fatty liver disease. *Clin Liver Dis* 2004; 8: 575-94.
- Abu-Abid S, Szold A, Klausner J. Obesity and cancer. *J Med* 2002; 33: 73-86.
- Neuschwander-Tetri BA. Nonalcoholic steatohepatitis. *Clin Liver Dis* 1998; 2: 149-73.
- Haynes P, Liangpunsakul S, Chalasani N. Nonalcoholic fatty liver disease in individuals with severe obesity. *Clin Liver Dis* 2004; 8: 535-47.
- Mori S, Yamasaki T, Sakaida I, et al. Hepatocellular carcinoma with nonalcoholic steatohepatitis. *J Gastroenterol* 2004; 39: 391-6.
- Bugianesi E, Manzini P, D'Antico S, et al. Relative contribution of iron burden, HFE mutations and insulin resistance to fibrosis in non alcoholic fatty liver. *Hepatology* 2004; 39: 179-87.
- Van Hoek B. Non-alcoholic fatty liver disease: a brief review. *Scand J Gastroenterol* 2004; 241: 56-9.
- Gundersen HJ. Stereology-or how figures for spatial shape and content are obtained by observation of structures in sections. *Microsc Acta* 1980; 83: 409-26.
- Mandarim-de-Lacerda CA. Stereological tools in biomedical research. *An Acad Bras Cienc* 2003; 75: 469-86.
- Petersen PM, Giwercman A, Pakkenberg B. Stereological methods as efficient and unbiased tools to quantitate structures in the testis. *Scand J Work Environ Health* 1999; 25: 31-3.
- Altunkaynak BZ, Ozbek E, Altunkaynak ME. A stereological and histological analysis of spleen on obese female rats, fed with high fat diet. *Saudi Med J* 2007; 28: 353-7.
- Reid AE. Nonalcoholic steatohepatitis. *Gastroenterology* 2001; 121: 710-23.
- Duran C, Aydinli B, Tokat Y, et al. Stereological evaluation of liver volume in living donor liver transplantation using MDCT via the Cavalieri method. *Liver Transpl* 2007; 13: 693-8.
- Aydinli B, Kantarci M, Polat KY, et al. Stereological evaluation of treatment response in patients with non-resectable hepatic alveolar echinococcosis using computed tomography via the Cavalieri method. *Liver Int* 2006; 26: 1234-40.
- Aguila MB, Pinheiro Ada R, Parente LB, Mandarim-de-Lacerda CA. Dietary effect of different high-fat diet on rat liver stereology. *Liver Int* 2003; 23: 363-70.
- Mathieu O, Cruz-Orive LM, Hoppeler H, Weibel ER. Measuring error and sampling variation in stereology: comparison of the efficiency of various methods of planar image analysis. *J Microsc* 1981; 121: 75-88.
- Gundersen HJ, Jensen EB, Kieu K, Nielsen J. The efficiency of systematic sampling in stereology--reconsidered. *J Microsc* 1999; 193: 199-211.
- Cruz-Orive LM, Weibel ER. Recent stereological methods for cell biology: a brief survey. *Am J Physiol* 1990; 258: 148-56.
- Odaci E, Sahin B, Sonmez OF, et al. Rapid estimation of the vertebral body volume: a combination of the Cavalieri principle and computed tomography images. *Eur J Radiol* 2003; 48: 316-26.
- Unal B, Özbek E, Aydin MD, et al. Effect of haloperidol on the numerical density of neurons and nuclear height in the rat hippocampus: a stereological and histopathological study. *Neurosci Res Commun* 2004; 34: 1-9.
- Gundersen HJ, Jensen EB. The efficiency of systematic sampling in stereology and its prediction. *J Microsc* 1987; 147: 229-63.
- Gundersen HJ. Stereology of arbitrary particles. A review of unbiased number and size estimators and the presentation of some new ones, in memory of William R. Thompson. *J Microsc* 1986; 143: 3-45.
- Sahin B, Emirzeoglu M, Uzun A, et al. Unbiased estimation of the liver volume by the Cavalieri principle using magnetic resonance images. *Eur J Radiol* 2003; 47: 164-70.
- Kiernan JA. *Histological and histochemical methods: theory and practice.* Oxford: Pergamon Press, 1990.
- Sterio DC. The unbiased estimation of number and sizes of arbitrary particles using the disector. *J Microsc* 1984; 134: 127-36.
- Christensen JR, Larsen KB, Lisanby SH, et al. Neocortical and hippocampal neuron and glial cell numbers in the rhesus monkey. *Anat Rec (Hoboken)* 2007; 290: 330-40.
- Kannekens EM, Murray RD, Howard CV, Currie J. A stereological method for estimating the fetomaternal exchange surface area in the bovine placenta at 135 days gestation. *Res Vet Sci* 2006; 81: 127-33.
- Shoelson SE, Herrero L, Naaz A. Obesity, inflammation, and insulin resistance. *Gastroenterology* 2007; 132: 2169-80.
- Nicol CJ, Adachi M, Akiyama TE, Gonzalez FJ. PPARgamma in endothelial cells influences high fat diet-induced hypertension. *Am J Hypertens* 2005; 18: 549-56.
- Duvnjak M, Virovic L. Non-alcoholic steatohepatitis. *Acta Med Croatica* 2003; 57: 189-99.
- Mendez-Sanchez N, Chavez-Tapia NC, Uribe M. Obesity and non-alcoholic steatohepatitis. *Gac Med Mex* 2004; 140: 67-72.
- Gilat T, Leikin-Frenkel A, Goldiner I, et al. Prevention of diet-induced fatty liver in experimental animals by the oral administration of a fatty acid bile acid conjugate (FABAC). *Hepatology* 2003; 38: 436-42.
- Vamecq J, Vallee L, de la Porte PL, et al. Effect of various n-3/n-6 fatty acid ratio contents of high fat diets on rat liver and heart peroxisomal and mitochondrial beta-oxidation. *Biochem Biophys Acta* 1993; 1170: 151-6.

34. Watanabe T, Tanaka Y. Age-related alterations in the size of human hepatocytes. A study of mononuclear and binucleate cells. *Virchows Arch B Cell Pathol Incl Mol Pathol* 1982; 39: 9-20.
35. Sanz N, Diez-Fernandez C, Cascales M. Variations of hepatic antioxidant systems and DNA ploidy in rats aged 2 to 8 months. *Biochim Biophys Acta* 1996; 1315: 123-30.
36. Kudryavtsev BN, Kudryavtseva MV, Sakuta GA, Stein GI. Human hepatocyte polyploidization kinetics in the course of life cycle. *Virchows Arch B Cell Pathol Incl Mol Pathol* 1993; 64: 387-93.
37. Saeter G, Lee CZ, Schwarze PE, et al. Changes in ploidy distributions in human liver carcinogenesis. *J Natl Cancer Inst* 1988; 80: 1480-5.
38. Yalçınkaya S, Unlüçerçi Y, Giriş M, et al. Oxidative and nitrosative stress and apoptosis in the liver of rats fed on high methionine diet: protective effect of taurine. *Nutrition* 2008; in press.
39. Natarajan SK, Eapen CE, Pullimood AB, Balasubramanian KA. Oxidative stress in experimental liver microvesicular steatosis: role of mitochondria and peroxisomes. *J Gastroenterol Hepatol* 2006; 2: 1240-9.
40. Abraham P, Wilfred G, Ramakrishna B. Oxidative damage to the hepatocellular proteins after chronic ethanol intake in the rat. *Clin Chim Acta* 2002; 325: 117-25.
41. Dai XF, Chen DF. Liver regenerative capacity after partial hepatectomy in rats with nonalcoholic fatty liver disease. *Zhonghua Gan Zang Bing Za Zhi* 2006; 14: 597-601.
42. Arvanitidis AP, Corbett D, Colbourne F. A high fat diet does not exacerbate CA1 injury and cognitive deficits following global ischemia in rats. *Brain Res* 2009; 1252: 192-200.
43. Mozaffari MS, Schaffer SW. Myocardial ischemic-reperfusion injury in a rat model of metabolic syndrome. *Obesity (Silver Spring)* 2008; 16: 2253-8.
44. Elahi MM, Cagampang FR, Mukhtar D, et al. Long-term maternal high-fat feeding from weaning through pregnancy and lactation predisposes offspring to hypertension, raised plasma lipids and fatty liver in mice. *Br J Nutr* 2009; 10: 1-6.
45. Duda MK, O'Shea KM, Lei B, et al. Low-carbohydrate/high-fat diet attenuates pressure overload-induced ventricular remodeling and dysfunction. *J Card Fail* 2008; 14: 327-35.
46. Duran C, Aydinli B, Tokat Y, et al. Stereological evaluation of liver volume in living donor liver transplantation using MDCT via the Cavalieri method. *Liver Transpl* 2007; 13: 693-8.
47. Aydinli B, Kantarci M, Polat KY, et al. Stereological evaluation of treatment response in patients with non-resectable hepatic alveolar echinococcosis using computed tomography via the Cavalieri method. *Liver Int* 2006; 26: 1234-40.